

Master sky images for the WFC3 G102 and G141 grisms

M. Kümmel, H. Kuntschner, J. R. Walsh, H. Bushouse
January 4, 2011

ABSTRACT

We have constructed master sky images for the WFC3 near-infrared G102 and G141 grisms using publicly available data. The method to generate the master sky images is presented. The quality of the master sky images is assessed by measuring the homogeneity of the background subtracted grism image. Data sets that had been used for constructing the master sky image show residuals of $\sim 0.7\%$ and $\sim 0.5\%$ of the sky brightness in G102 and G141, respectively. Other G141 data that were obtained several months later show larger residuals of $\sim 1.1\%$ of the sky brightness, which indicates a possible variability of the grism background image shape as a function of time. The average sky brightness measured in the G102 and G141 images is $0.83\text{e}^-/\text{s}$ and $1.32\text{e}^-/\text{s}$, respectively.

1. Introduction

The Wide Field Camera 3 (WFC3) IR channel is fitted with two grisms for slitless spectroscopy: G102 for the shorter (800-1150nm; 2.45nm/pix) and G141 for the longer (1100-1700nm; 4.65nm/pix) NIR wavelengths (Kuntschner et al. 2010, Walsh et al. 2010). As can be seen in the upper panels of Figure 1 on the example images 'ib6o21qmq_flt.fits' (G102) and 'ib6o23rsq_flt.fits' (G141), the sky background in these slitless spectroscopy modes shows some distinct, non-uniform features. There is the circular region with little or no sensitivity around $(x, y) = (300, 50)$ (the so-called “Death Star”) and the feature at the right border

called the 'wagon wheel', both of which also appear in direct images because they are intrinsic to the detector. The main feature exclusive to grism data is a slowly varying profile as a function of the x-coordinate. This profile is clearly visible in the lower panels in Fig. 1, which show a median-combined selection of rows that do not contain any object signatures. This profile is produced by the overlay of the various orders ($+1^{\text{st}}$, 0^{th} , $+2^{\text{nd}}$, -1^{st} ...) of dispersed background light. Due to the finite entrance pupil of the telescope, higher orders of background light do not contribute at certain positions in the dispersion (x) direction and thus result in a drop in the combined background light near the left and right edges of images.

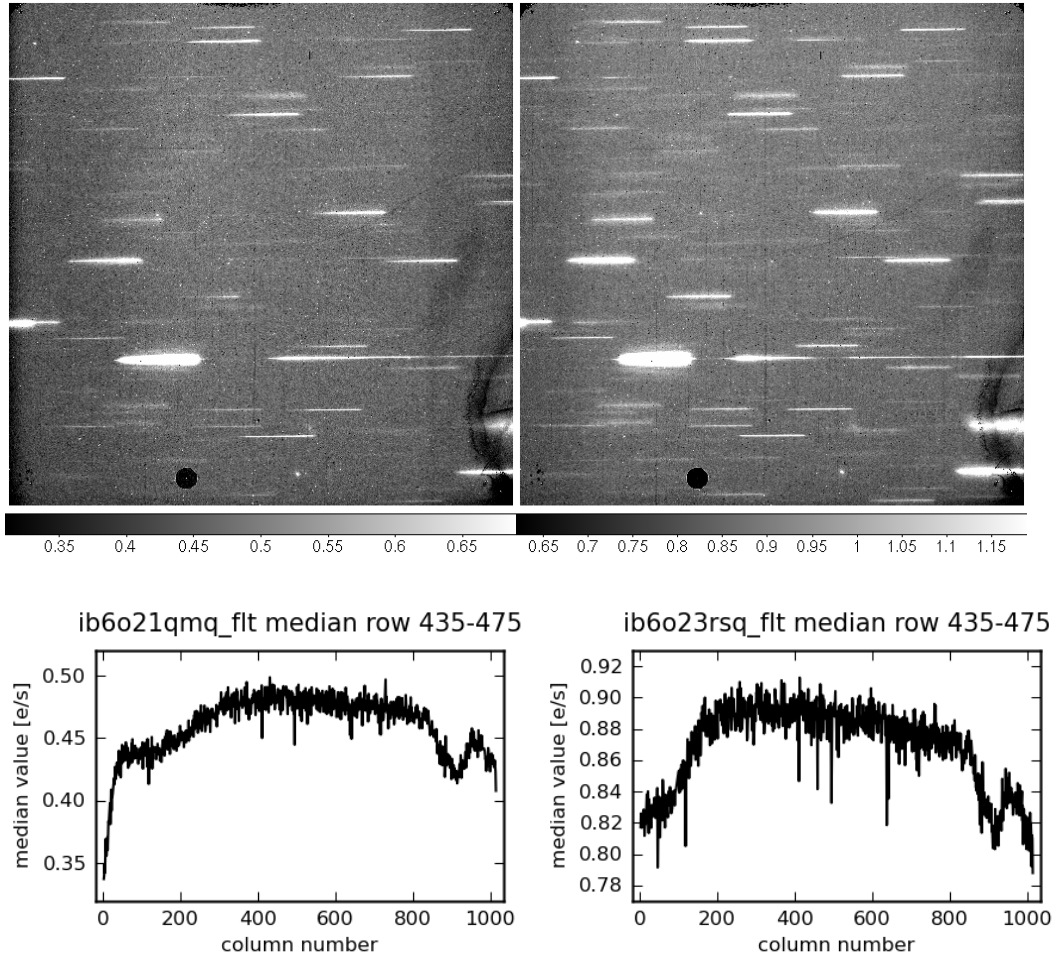


Figure 1: The upper panels show two WFC3/IR grism images 'ib6o21qmq_flt.fits' (G102, left) and 'ib6o23rsq_flt.fits' (G141, right). Besides detector features, such as the dead spot at the bottom centre and the 'wagon wheel' at the right, the dominant large-scale background structure is a profile that varies as a function of the x-coordinate. This variation is demonstrated in the lower panels, which show a median-combined set of rows (435-475) that do not contain any object traces.

Accurate sky background removal is a key element for the extraction of faint spectra from slitless spectroscopic data. For both the ACS/G800L and NICMOS/G141 slitless spectroscopic modes, good results have been achieved by scaling a slitless master sky image to the background level of each science image and then subtracting the sky background globally (this technique was performed for the GRAPES: Pirzkal et al 2004, PEARs: Malhotra et al. 2009 and NICMOS/HLA: Freudling et al. 2008 programs). This ISR presents master sky images for the WFC3 G102 and G141 grism modes that have been generated from publicly available data taken in the period October 2009 - March 2010. Section 2 reports the methods applied to generate the master sky images. Section 3 discusses the accuracy of the background subtraction that can be achieved with the master sky images. Section 4 summarizes the results.

2. Producing the G102 and G141 master sky images

We used a set of 105 and 100 publicly available science images observed from October 2009 to March 2010 for G102 and G141, respectively, as input for the generation of the master sky images. The data were taken as part of the programs 11359 (PI: O'Connel), 11600 (PI: Weiner) and 11696 (PI: Malkan). The basic method of producing a master sky image from a set of science exposures is to combine the sky areas (the regions free of object spectra) in slitless spectrum images. In order to achieve this one has to:

- scale the science exposures to the same sky level;
- combine the scaled exposures such that object signatures are removed.

In order to avoid any possible bias when combining the scaled values for each pixel to a representative master sky value and thus avoid a bias in the master sky, we have refined this basic method in various respects:

- areas that are known to be covered by an object are masked out when combining the scaled images;
- pixels with data quality issues (being e.g. 'bad' or 'unstable' or 'hot') in the associated DQ array are masked out when combining the scaled images;
- the scaling value is determined by fitting the equation $y = m \cdot x$ to the set of tuples (x_i, y_i) , where y_i is a pixel value in the science image and x_i the value of the same pixel in a master image used for the scaling. A robust value for m is derived with several kappa-sigma clipping iterations in the fitting process. For curved surfaces, such as the WFC3/IR background, this scaling promises a higher accuracy than a simple 'median' or 'average' estimated over a certain image area.

To produce the master sky images the set of G102 and G141 science images were processed as follows:

- the science images were grouped into "associations" (Freudling et al 2008, Kümmerle et al. 2011), i.e. independent sets of images that cover the same area on the sky and usually were observed in a sequence;
- for each set of grism images and their associated direct images, a basic spectral extraction was performed using the aXe task **"axecore"**. The primary purpose of this step is to generate the mask images that are produced as part of the contamination assessment for each grism image (with parameter **contam="geom"**) and mark the position of the spectral orders of all objects on the grism image;
- using the mask image and the data quality array, the scaling factor of each grism image against a fixed master image for scaling is determined using the method explained above;
- each grism image is divided by its scaling factor. Pixels that were masked in the scale determination are also masked;
- each set of scaled grism images is combined with the IRAF task **"imcombine"** to form a master sky image for each grism; in order to remove object signatures that were not covered in the corresponding mask or other spurious pixel values, the task is run with the clipping and combine parameters **combine='median', reject='avsigclip', mclip='YES', lsigma=4.0, hsigma=3.0**.

These processing steps were iterated several times, using an arbitrary grism image as a scaling image on the first run and then the master sky image resulting from the previous iteration in subsequent runs. The resulting master sky images for the G102 and G141 grisms are shown in Figure 2. The scaling image used in each iteration and the final master sky images were normalized to a median level of 1.0, which is mandatory in order to get correct noise estimates in the spectral extraction when using the master sky image in the aXe task **"axeprep"**. The scaling factor determined for each grism image corresponds to the sky background level in that image (in e^-/s). Thus a side result of generating the master sky images is the background level in each data set whose sky background is fitted. A plot of the sky levels in these sets of images is shown in Figure 3 as a function of MJD.

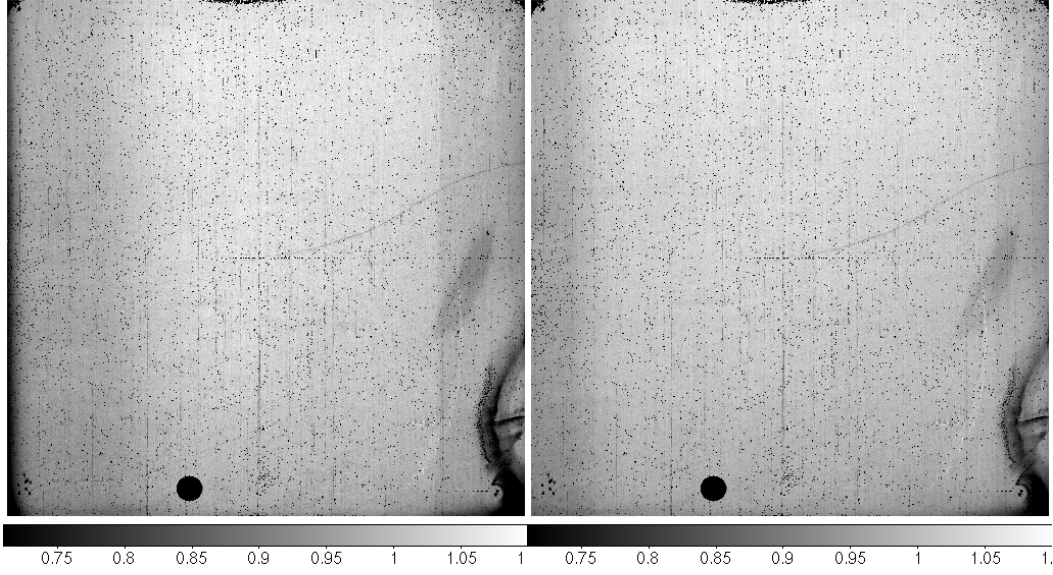


Figure 2: The two master sky images for the G102 (left) and the G141 (right) grisms, derived from ~ 100 science images per grism.

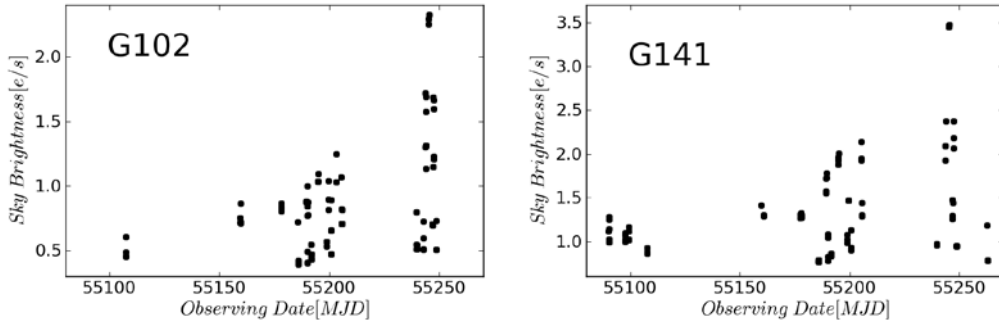


Figure 3: The sky brightness values of the two near-infrared grisms, measured in the science images, as a result of the image scaling. The G102 background values are in the range 0.40-2.32e/s with an average of 0.83e/s, the G141 values cover the range 0.77-3.48e/s with an average of 1.32e/s.

3. Quality of the G102 and G141 master sky images

To estimate the quality of the G102 and G141 master sky images, we applied them in a standard data reduction with aXe, e.g. for the data from the Early Release Science (ERS) grism field (observed in October 2009, see Straughn et al. 2011). Figure 4 shows examples of the background subtracted science images ‘ib6o21qmq_flt.fits’ (G102) and ‘ib6o23rsq_flt.fits’ (G141), which are displayed before background subtraction in Figure 1. There are no residuals that could obviously be attributed to an insufficient background subtraction. As a further test we identified on both images some rows that are apparently void of any object

trace and evaluated the residual sky background by median-combining these rows. Because the G102 and G141 example images chosen here correspond to the same area on the sky, the rows 435-475 can be used for both. Figure 5 shows these sky spectra: on the left side for ‘ib6o21qmq’ and on the right side for ‘ib6o23rsq’ (the lower panels in Figure 1 show the same median-combined rows with background). The red lines display a smoothed version of the residual sky, derived by averaging the median-combined sky in a running window of 30 pixel width. The rms in the data shown as black lines are 0.0048 and 0.0056 e⁻/s for G102 (left panel) and G141 (right panel), respectively, which corresponds to 1.0% and 0.64% of the original sky background level.

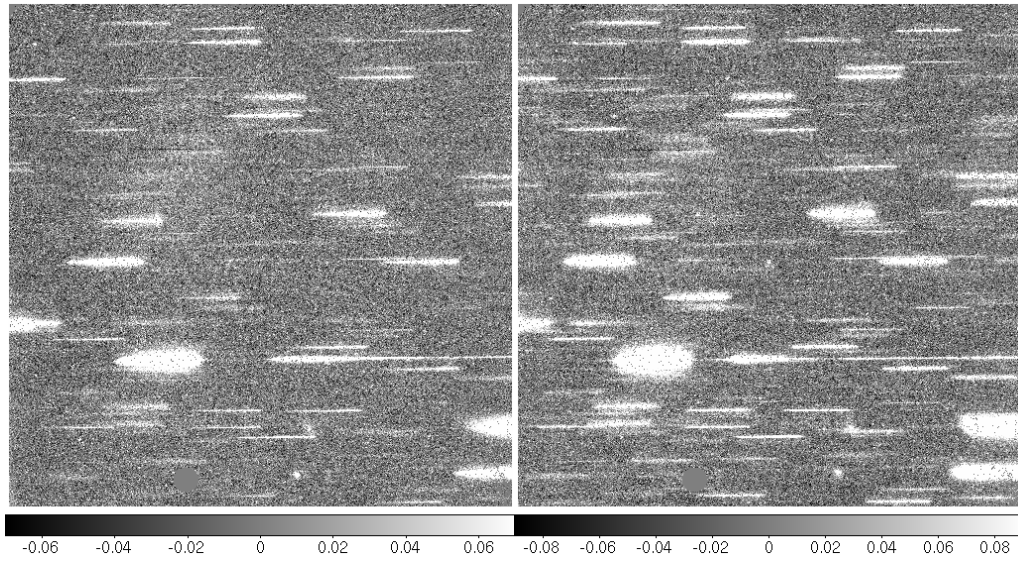


Figure 4: The background subtracted images ‘ib6o21qmq_flt.fits’ (G102, left) and ‘ib6o23rsq_flt.fits’ (G141, right). The background removal (0.46 e/s in G102 and 0.8 e/s in G141) was done with the aXe task “axeprep” using the master sky images shown in Fig. 2.

Because the WFC3/IR grism background could be variable with time or with the sky background level, we also applied our master sky images to a dataset obtained in February 2010 at a much higher sky level. Figure 6 shows the background subtracted science images ‘ib8cejt0q’ (left, G102) and ‘ib8cejt4q’ (right, G141) and Figure 7 shows a median-combined section of rows with no object traces. The red lines again display a smoothed version of the residual sky, derived by averaging the median-combined sky in a running window of 30 pixel width. Figure 6 does not reveal any significant failure of the background removal at that epoch and high sky background level. In Figure 7 the combined rows (black lines) have an rms of 0.009 and 0.012 e⁻/s in G102 and G141, respectively. While the absolute values of the residuals and their rms are clearly larger than in Figure 5, the relative accuracy of the sky subtraction, evaluated as the rms divided by the background level, is at an even lower level of 0.40% and 0.35%.

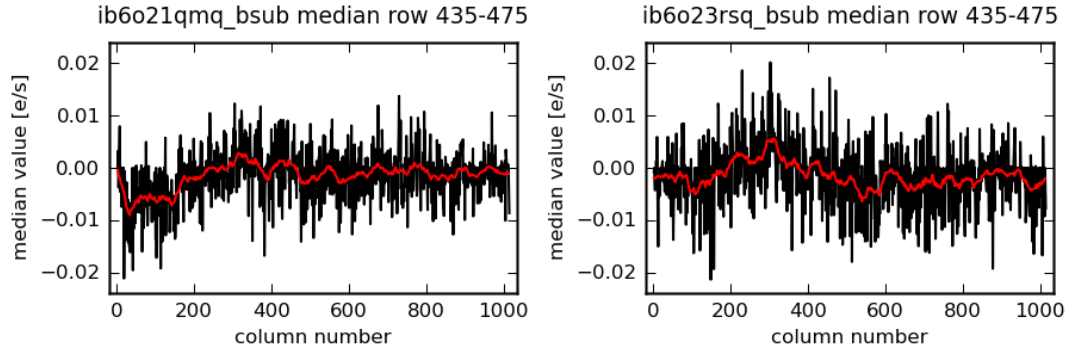


Figure 5: A median-combined set of rows (435-475) without any object beams in them, derived from the background subtracted images (see Figure 4)) ‘ib6o21qmq_flt.fits’ (left, G102), and ‘ib6o23rst_flt.fits’ (right, G141). The red lines in the lower panels show the smoothed background, computed by averaging in a running window of 30 pixel width.

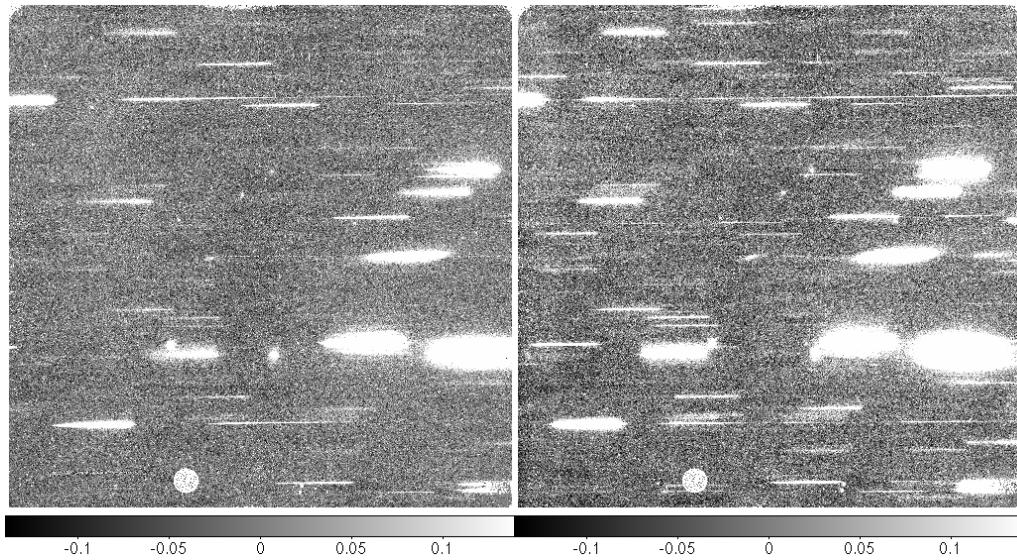


Figure 6: The background subtracted images ‘ib8cejt0q_flt.fits’ (G102, left) and ‘ib8cejt0q_flt.fits’ (G141, right). The removal of the high sky background (2.30 e/s in G102 and 3.46 e/s in G141) was done with the aXe task “axeprep” using the master sky images shown in Fig. 2.

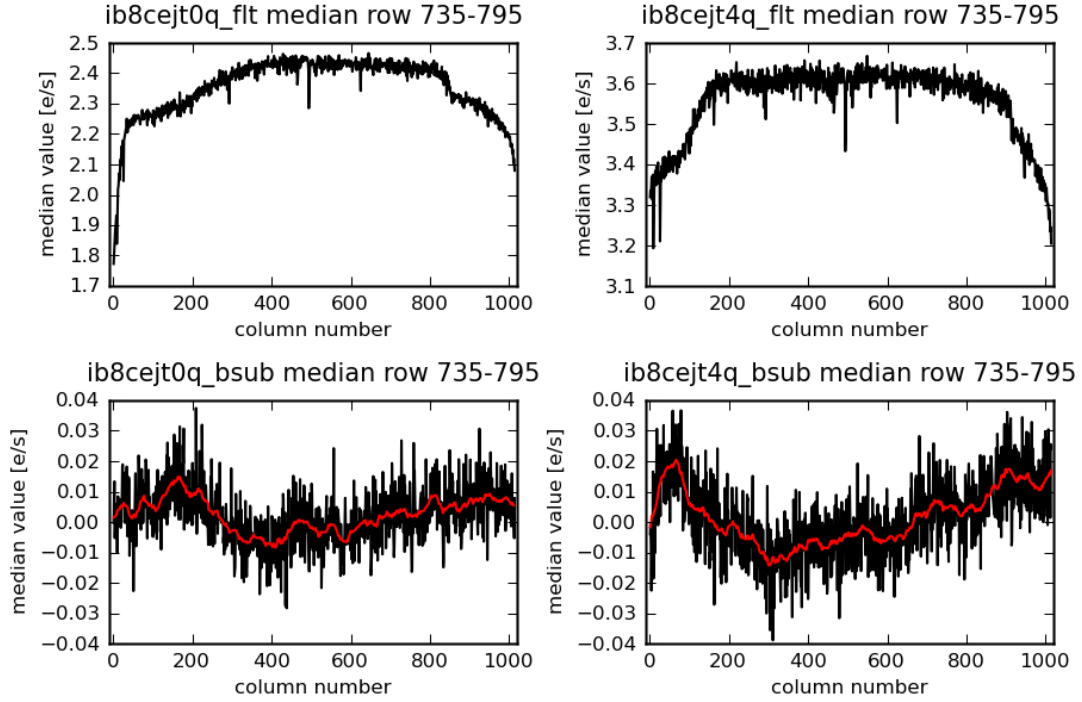


Figure 7: A median-combined set of rows (735-795) without any object beams in them for images *ib8cejt0q_flt.fits* (G102) and *ib8cejt4q_flt.fits* (G141). The upper panels are for the original images and the lower ones are the background-subtracted images (Figure 6). The red lines in the lower panels show the smoothed background, computed by averaging in a running window of 30 pixel width.

To further explore the long-term stability of the master sky images, we applied the G141 background image to a dataset taken as part of the program 12099 (PI: Riess), which was obtained at the end of October 2010 and thus more than half a year later than the science images that were used for constructing the master sky image. Figure 8 shows an example of the entire background-subtracted science image ‘ibfup3xq’. Figure 9 displays a median-combined section of rows with no bright object traces with the black line and its smoothed version with the red line. In general, the background subtraction works remarkably well over the entire Field-of-View (FOV), however the relative residuals in Fig. 9 are 1.1% of the sky brightness ($\text{rms}=0.0096 \text{ e}^-/\text{s}$), which is larger than the corresponding values in the two previous examples for G141. While it is very difficult to find truly empty rows on a typical WFC/IR slitless image, and thus the residuals might be too large due to faint object traces, this may indicate a variability of the sky background shape at the level of a percent on timescales of a year, and suggests that master sky images covering restricted time spans may need to be constructed for the highest fidelity background removal.

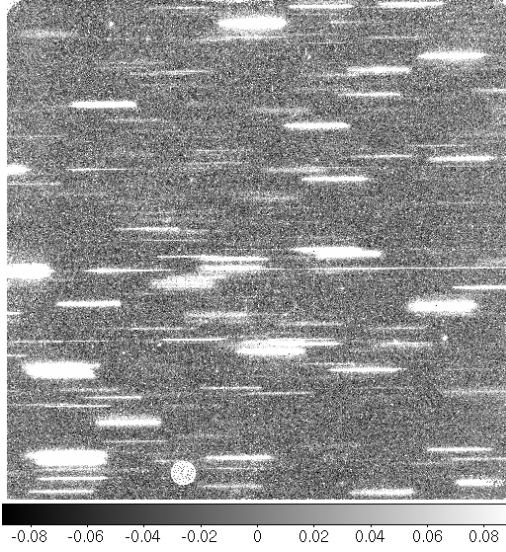


Figure 8: The background subtracted image ‘ibfup3rxq_flt.fits’ (G141). The removal of the sky background (0.89e/s) was done with the aXe task “axeprep” using the master sky images shown in Fig. 2.

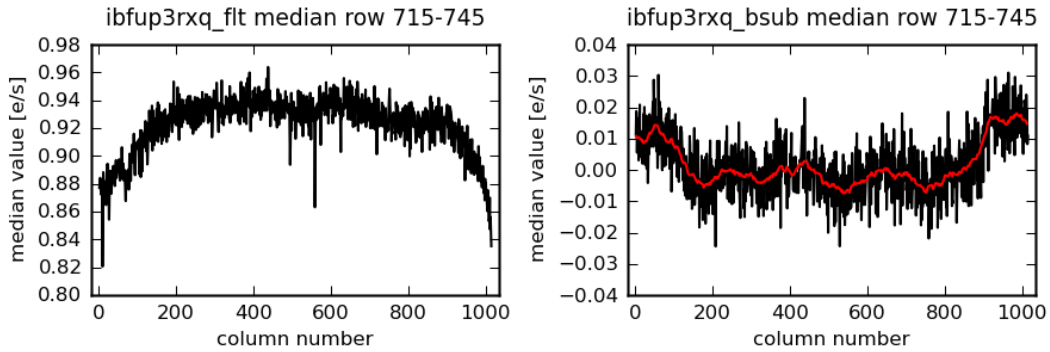


Figure 9: A median-combined set of rows (715-745) without any object beams in them from the image *ibfup3rxq_flt.fits* (G141). The left panel was derived from the original *flt* images, the right panel from the background-subtracted images (Figure 8). The red line in the right panel shows the smoothed background, computed by averaging in a running window of 30 pixel width.

4. Summary and outlook

We have constructed master sky images for the WFC3/IR grisms G102 and G141 by evaluating, for each grism, ~ 100 publically available science images that were observed between October 2009 and March 2010. For two examples of science data taken within this period, the master sky images remove the background globally to an accuracy of $\sim 0.7\%$ and $\sim 0.5\%$ of the sky brightness in G102 and G141, respectively. For a G141 science image observed half a year after the time

interval over which the master sky images were obtained we found larger residuals of ~1.1% of the sky brightness, which may indicate a possible variability of the sky background shape on timescales of a year.

The growing amount of available data in the WFC3 G102 and G141 slitless modes should soon allow a more detailed investigation of the parameters that influence the shape of the grism background and may result in a series of master sky images that are adjusted to specific epochs or conditions. Observers may also try to create master sky images that are derived from or adjusted to their own data using the techniques described here, in order to obtain smaller sky residuals. Our experience suggests that at least ~30 science images are needed to be combined to yield a master sky image without any object traces affecting it.

Our G102 and G141 master sky images, named WFC3.IR.G102.sky.V1.0.fits and WFC3.IR.G141.sky.V1.0.fits, are available for download at:

http://www.stsci.edu/hst/wfc3/analysis/grism_obs/. The images can be used as input to the task **"axeprep"** in the aXe spectral extraction software (Kümmel et al. 2009) to globally subtract the background from slitless data taken with the corresponding grism.

References

- Freudling, W., Kümmel, M., Haase, J., et al. 2008, A&A 490, 1165
- Kümmel, M., Walsh, J. R., Pirzkal, N., Kuntschner, H., & Pasquali, A. 2009, PASP, 121, 59
- Kümmel, M., Kuntschner, H., Walsh, J. R., & Bushouse, H. 2010, in The 2010 HST Calibration Workshop, edited by S. Deustua, & C. Oliveira
- Kümmel, M., Rosati, P., et al. 2011, submitted to A&A
- Kuntschner, M., Kümmel, M., Walsh, J.R. 2010, The WFC3 IR Grism Data Reduction Cookbook,
http://www.stsci.edu/hst/wfc3/documents/WFC3_aXe_cookbook.pdf
- Rhoads, J.E., Malhotra, S., Pirzkal, N., et al. 2009, ApJ 697, 942
- Pirzkal, N., Xu, C., Malhotra, S., et al. 2004, ApJS 154, 501
- Straughn, A.N., Kuntschner, H., Kümmel, M., et al. 2011, AJ 141, 14